Proceedings of ASME Turbo Expo 2017
GT2017
June 26-30, 2017, Charolette, USA

GT2017-63807

DEVELOPMENT OF A COMBINED EDDY CURRENT AND PRESSURE SENSOR FOR GAS TURBINE BLADE HEALTH MONITORING

V. Sridhar and K. S. Chana
Osney Thermo Fluids Research Laboratory
Department of Engineering Science
University of Oxford
Oxford, United Kingdom

ABSTRACT

Gas turbine engine health monitoring systems play an active role to ensure timely maintenance and prevention of failures. Tip-timing and tip clearance measurements form a major part of gas turbine health monitoring systems. They are used to assess turbomachinery blade vibrations using non-contact systems such as optical, capacitive, Hall Effect, eddy current etc. Most of these sensors are prone to contamination, non-linearity and cannot measure both tip-timing and tip-clearance together. Eddy current sensors are found to be robust and can measure both tip-timing and tip-clearance at the same time. They are already being used in gas turbine health monitoring systems to assess compressor and turbine blade vibrations. Apart from assessing blade vibrations, it will be quite beneficial to predict and prevent surge and stall of compressors in an engine. Surge and stall can be disastrous for an aircraft during flight as it can cause severe damage to the engine. Pressure sensors are generally used to study the variations in the inlet flow for surge and stall protection in an engine and play an important role in health monitoring.

A new combined sensor that can measure tip-timing, tip-clearance and pressure is developed at the University of Oxford for use in gas turbine engine health monitoring. The combined sensor uses a pressure sensor in the centre and is enclosed by an eddy current sensor forming a compact single package. The sensor is found to be quite robust and is able to operate in these harsh environments without any loss in accuracy. The pressure sensor used here is a fast response optical based sensor that is known to work at high temperatures and is less noisy compared to piezo based pressure sensors. The pressure sensor can also measure the steady state temperature of the casing.

The paper presents the development of this combined sensor along with experimental results of tip-timing, tip clearance and unsteady pressure measurements carried out on a jet engine fan blades that was tested from idle to full speed. The engine tests comprised of looking at the effects of squeezing the inlet casing during the run in order to cause a tip rub on blade vibrations. Tests were also conducted to study the effect of distortions in the inlet flow on blade vibrations by placing varying number of bars in front of the inlet of the engine.

INTRODUCTION

Active health monitoring forms a important part of the aircraft systems. Health monitoring of gas turbine components ensures timely maintenance by detection of potential failures and thus reducing unnecessary down time. Blades of a gas turbine engine are subjected to vibrations caused by dynamic loads such as rotor imbalances, varying blade tip clearance due to non-concentric casings, distortions in the inlet flow (caused by irregular intake geometries). These can damage the blades and can lead to aerodynamic forcing causing high cycle fatigue. This has a major impact on safety and whole life costs. Detection of the changes in blade vibration modes and levels due to damage or deterioration would allow improvements to the inspection, repair and replacement process.

Blade Tip-Timing (BTT) and tip-clearance measurements

are routinely used to monitor engine blades for vibrations. Some of the methods used to do these measurements involve the use of optical probes, eddy current, capacitive, Hall effect sensors etc. [1], [2], [3], [4]. All these sensors measure the arrival time of the blades and some can measure the tip-clearance (eddy current and capacitance).

The eddy current sensor is the most robust and immune to contaminations when compared with industry standard optical probes. They are already being used in gas turbine power generation for in-service health monitoring on first stage compressor blades and on the last stage of steam turbine blades, whereas, the other type of sensors are still used on developmental engines due to their limitations.

The aim of this research is to show the performance and accuracy of a newly developed combined pressure and eddy current sensor and its application in measuring tip-timing in the fan stage of a small gas turbine engine.

Experimental Setup

Experimental measurements were carried out using the combined pressure and eddy current sensor developed at the University of Oxford and Oxsensis® as shown in Fig. 1a. The sensor has a diameter of 13 mm and six sensors were used for the measurements along the 180 degree of the circumference.

The combined probes were manufactured in peek Polyether Ether Ketone (a semi crystalline organic polyether thermoplastic) which is an aerospace approved material. The probe has a temperature capability of 250°C continuous and 320°C intermittent. However, the sensor is actually capable of operating at higher temperatures around 500 to 600°C with different probe materials. The probe has a diameter of 13 mm.

The Oxsensis® pressure sensor is used for monitoring dynamic pressures in harsh environmental conditions with temperatures up to 1000°C at the tip of the sensor. The transducer element uses an optical Fabry-Perot cavity made from crystalline sapphire. The sapphire membrane is deflected under the influence of the pressure to be measured and the corresponding change in cavity size is detected optically using interferometry. A dual wavelength scheme is employed to eliminate adverse effects of fibre bending losses that may occur in a high-vibration environment. The sensor can also provide temperature as an additional parameter of interest which allows compensating for the thermally induced changes in cavity size and thus, enabling the measurement of (quasi)-static pressure at the same time. The enhanced sensor has an accuracy of $< 2\%$FS. The Oxsensis® signal processing unit combines all of the optical components with the required electronics to produce a calibrated pressure output.

Six probes were fitted to the casing of the fan over the first stage fan blade as shown in Fig. 1b. Figure 1c shows the sensor locations around the casing from the top dead centre position.

(a) Combined sensor

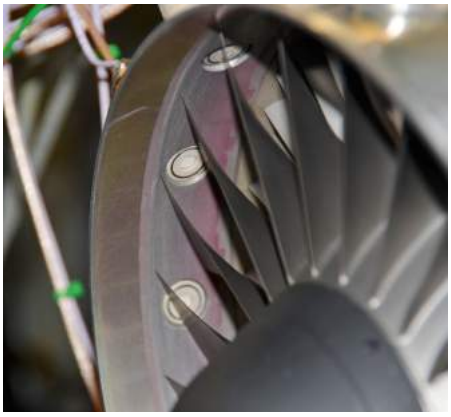

(b) Sensor on the engine

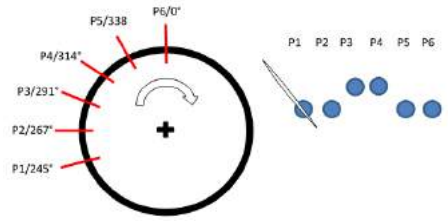

(c) Locations of the sensors on the engine

(d) T3 and Monitoring box

FIGURE 1: Combined sensor and mounting

Probe 1 was located at 245° and Probe 6 at 0°. Probes 3 and 4 were not moved forward as the casing squeeze mechanism bars prevented these probes from being fitted at a more forward location.

The eddy current sensor part of the probe goes to a small electronics box called the turbine-tip-timing unit (T3) (Fig. 1d). The T3 box drives the probe and also processes the signal in a manner that it separates the tip clearance from the blade arrival time information. The T3 outputs time of arrival trigger pulse, the raw eddy current sensor signal and scaled tip clearance. The T3 output is then sent to a tip-timing PC.

For the dynamic pressure part of the probe, the signal is transmitted via a standard fibre optic cable to an Oxsensis signal conditioning and driver box and then the output from the box is fed to a National Instruments high speed DAQ. The data was sampled at 1 MS/s per channel. The probe cable was extended using standard 12 m fibre extension cables to reach the control room where the electronics were situated. The 12 m fibre extensions did not degrade the signal quality.

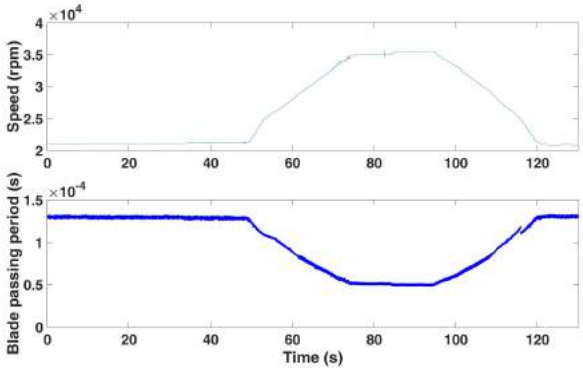

FIGURE 2: A typical run profile

A typical engine run is shown in Fig. 2. It consists of idling for few minutes and throttling up and maintaining full speed for couple of seconds and then again throttling down. The engine idles at 20000 rpm and the max rpm is 35000. The lower trace shows tip timing data given as blade arrival time. The trace is a mirror image of the engine LP shaft speed,as the engine speed increases, the time between blades gets shorter. This is recorded directly from the T3 box which processes the signal to blade arrival time in analogue electronics. At around 25,000 rpm there is a discontinuity in the data, the cause of this is not obvious. The T3 electronics are optimised for a maximum speed that is much lower in blade passing periods than the small gas turbine engine as it was developed for large industrial and large aerospace gas turbines. The electronics were modified for the engine to cope with the significantly higher blade passing frequencies, basic validation was carried out for the engine test but time precluded extensive testing, hence this could be a possible cause.

Results and discussion

Several tests were carried out to study the effect of squeezing the casing in order to cause a tip rub and the effect of inlet distorted flow on vibrations.

Effect of squeezing the casing

One of the faults implemented in the engine run was to understand the effect of tip rub by squeezing the casing to create a fan blade tip rub on the casing. The aim was to compare the data without casing distortion followed by a test where the casing was squeezed at two opposite points to introduce casing distortion such that a fan rotor tip rub was induced. The squeeze was initially done at idle speed and the engine was then taken to full operating speed with the casing squeezed.

The mechanism used to distort the casing is shown in Fig. 3, where a hydraulic ram is fitted to the casing at about the 2 o'clock position with a frame that fits around the casing and anchors on the opposite side. The anticipation was that the casing would be squeezed and a rotor tip rub would be induced in the region of probe 6 at the 0° position where probe 6 was mounted and, depending on the stiffness of the casing an increase in diameter may be experienced at 90° from the squeeze point. Surprisingly during the squeeze process, the eddy current part of the combined probe at location 6, nearest the squeeze region, showed an increase in tip clearance rather than a reduction. This was monitored in real time and this entailed that the squeeze process had increased the diameter of the casing at the probe 6 location as opposed to reducing it. Following the initial test, the casing was left in the squeeze position and the clearance measured around the casing between the fan blade tip and the casing had increased at the probe 6 location, reduced at the hydraulic ram location to a point where the blade was touching the casing and remained similar elsewhere around the annulus. At the probe 6 location the clearance had grown by 30 thou and explained the sensor measuring an increased clearance. The reason for the increase is that as the casing was squeezed it caused it to distort only locally in a manner where it became "M" shaped i.e. reduced in the centre of the squeeze location and raised just to the sides.

Figures 4a and 4b presents the measured blade deflection for successive rotations for a datum run and a run with the fan blade tip rubbing. For each blade the average shown as the red dot is calculated for the all the revolutions and the arrival is given for every revolution. The results show that the blade deflection scatter from revolution to revolution increases significantly for the tip rub case. The data presented here are taken from only probe number 6, the probe closest to the squeeze area. The blade deflection from rev to rev is within the range of about $\pm 0.2mm$

FIGURE 3: Hydraulic ram to squeeze the casing

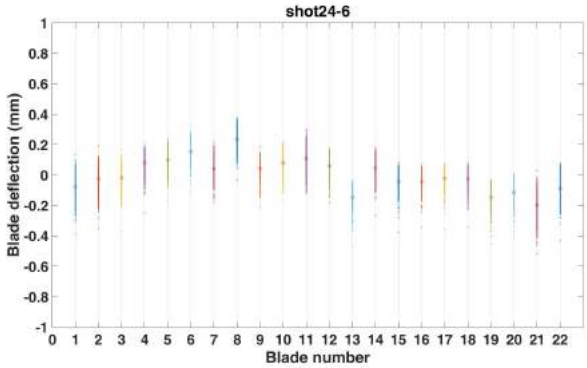

(a) No squeeze

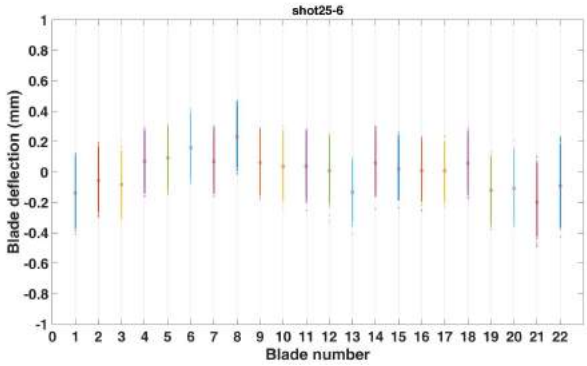

(b) Squeeze

FIGURE 4: Deflection before and after squeezing

whereas for the tip rub case, the measurements are in excess of $\pm 0.4mm$. The average position of the blades with respect to each other is similar for the two cases. This data was taken with the engine at idle operation where the tip rub was initiated.

Raw pressure signals taken from sensor 1 and 6 with and without squeezing the casing are as shown in Figs. 5a and 5a. At the horizontal position near probe 1 a small decrease in the casing pressure is experienced as the casing is slightly forced into an oval shape increasing the diameter at the plane normal to the squeeze axis near probe 1. In figure 5b, with the squeeze at its full extent at the probe 6 location, the pressure reduces significantly with squeeze.

Inlet distortion of flow

The inlet aerodynamic distortion tests were performed by introducing a set of bars fitted in the inlet duct of the engine upstream of the fan blade row. Three rings were tested separately that contained 7, 13 and 19 bars (Fig. 6). The bars are in aerofoil shape with the thicker section downstream to produce a thicker wake in the flow. Figure 7 shows the engine fitted with the 19 bar ring, the rings have a hub and casing circular ring interconnected with a series of bars that are profiled in shape.

Figure 8 shows the blade tip deflection for each blade for each revolution and an average over the run duration. The results processed for this data are taken during the acceleration part of the engine run. Notably the blade tip deflection for the uniform inlet without distortion (Fig. 8a) shows a significantly smaller blade tip deflection range in comparison to the results with the inlet distortions. The blade tip deflection for bar 7 (Fig. 8b) is also similar to the no bar case but then increases with bar 13 (Fig. 8c) and 19 (Fig. 8d).

Using the tip timing data a waterfall plot is created showing each blade on the y-axis and engine speed on the x-axis as shown in Fig. 9. The blade deflection is scaled and shown in the vertical plane for each blade trace. As the engine is accelerated from idle to full operating speed, the points at which the blade experiences a resonance can be easily seen using this type of plot. Figure 9a shows the results for the uniform inlet case where there is no inlet distortion introduced, just after 23,000 rpm all blades experience a resonance which seems to be the blade or rotating

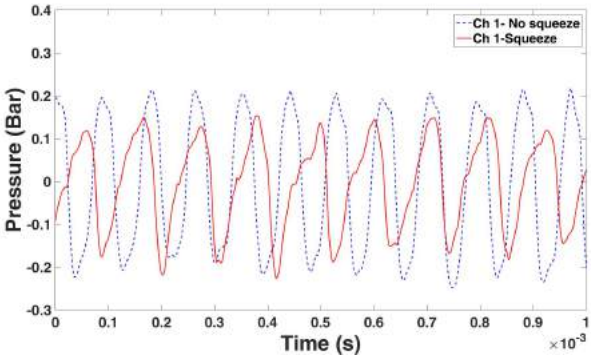

(a) Pressure sensor 1

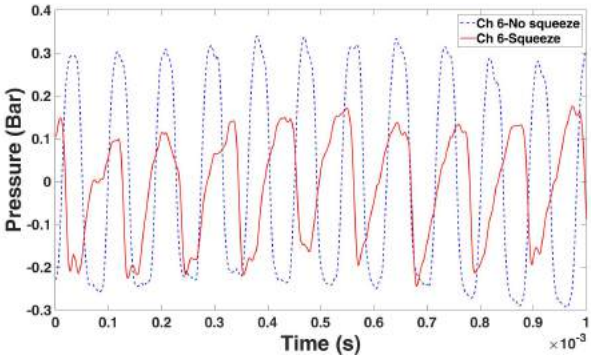

(b) Pressure sensor 6

FIGURE 5: Pressure change before and after squeezing

assembly's natural resonance, usually linked to blade flutter. At around 26,500 rpm the blades experience a further resonance until around 28,000 rpm. The largest resonance is noted at just before 29,000 rpm which ends at around 29,500 rpm.

Similar waterfall plots are given for 7, 13 and 19 bars (Figs. 9b to 9d), showing the resonances with respect to engine speed. All this data has been derived from a single probe (probe 6). We observe that with the inlet distortion of the flow, the resonance with 7 bars is similar to that with no-bars but increases significantly for 13 bars and 19 bars. An interesting thing to note is the resonance occurring at 23000 RPM in the case of no bars remains the same for 7 bars but shifts to $\approx$ 24000 RPM for 13 and 19 bars. The increase in resonances for 13 and 19 bars also explains the increase in deflections observed earlier.

Figure 10 shows the unsteady casing pressures for the uniform undisturbed inlet, 7 bar, 13 bar and 19 bar inlet distortion from the combined pressure and tip timing probes 1 and 6. Surprisingly the unsteady pressure levels for the 7 bar distortion ring are significantly smaller than the uniform. The reason for this is unclear but could possibly be due to the blockage of the bars being in direct alignment with sensors 1 and 6. At the probe 1 location , the differences in casing pressure are small. However,

(a) 7 Bars

(b) 13 Bars

(c) 19 Bars

FIGURE 6: Bars used in the experiments for inlet distortion

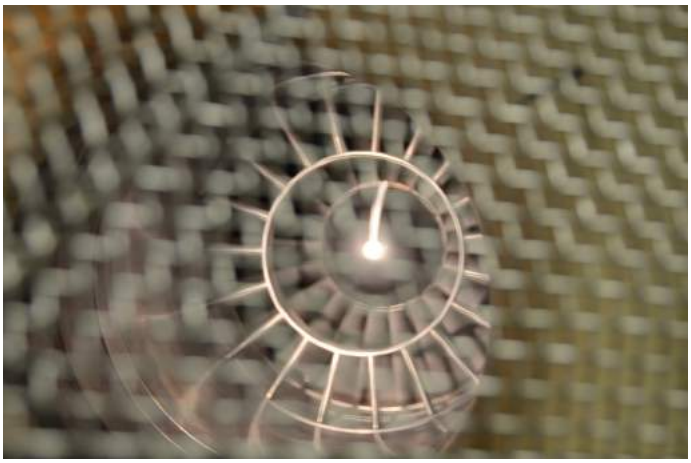

FIGURE 7: Engine inlet with bars in the front

at probe 6 location with uniform inlet, in general, has a larger peak to peak amplitude than the inlet distortion cases.

Conclusions

A new combined pressure and eddy current sensor is developed for tip-timing, tip-clearance and pressure measurement applications. The sensor was tested on the fan stage of an actual gas turbine engine and found to work quite well. The results showed the effect of squeezing the casing. The results for both the fan blade tip deflection and casing unsteady pressures showing that the combined sensor detects the inlet distortion introduced with the bars, very well in terms of the blade tip deflection, blade resonance induced and the changes in the casing time resolved static pressure. The deflections and resonances were also detected in real time using the BTT system during the test.

Acknowledgement

The authors would like to acknowledge Jonathan Sullivan for his help in carrying out the experiments.

REFERENCES

[1] Flotow, A. V., Mercadal, M., and Tappert, P., 2000. "Health monitoring and prognostics of blades and disks with blade tip sensors". In Proceedings of IEEE Aerospace Conference, Vol. 6, pp. 433–440.

[2] Lattime, S. B., and Steinetz, B. M., 2009. "Turbine engine clearance control systems: Current practices and future directions". In 38th Joint Propulsion Conference and Exhibit cosponsored by AIAA, ASME, SAE, and 47th AIAA Aerospace Sciences Meeting Including The New Horizons

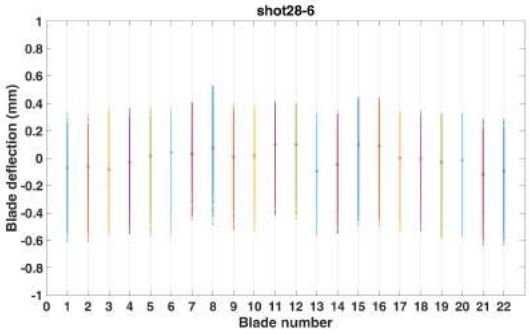

(a) No bars

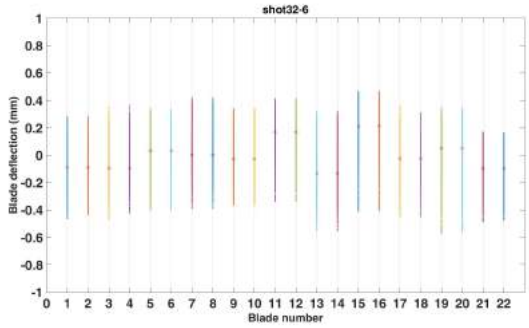

(b) 7 bars

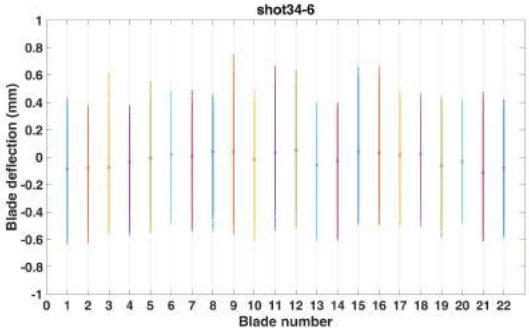

(c) 13 bars

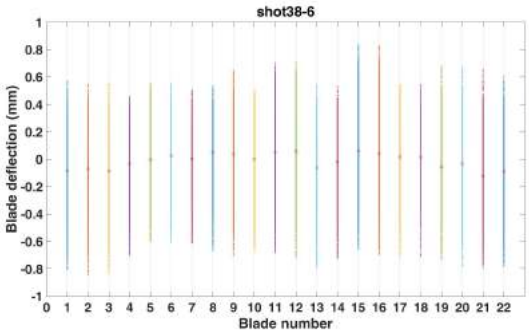

(d) 19 bars

FIGURE 8: Deflections with and without bars

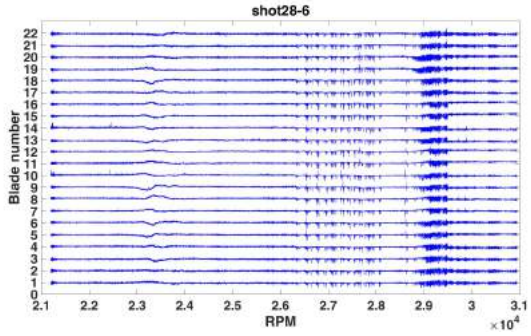

(a) No bars

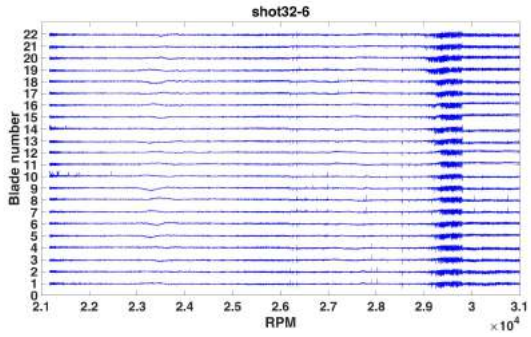

(b) 7 bars

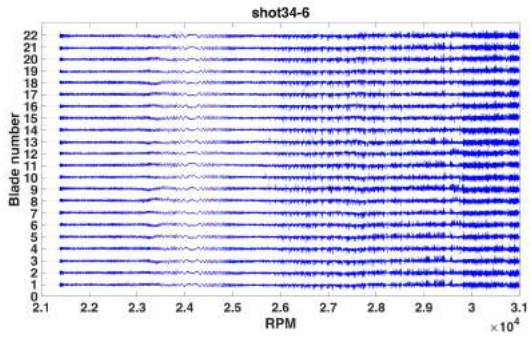

(c) 13 bars

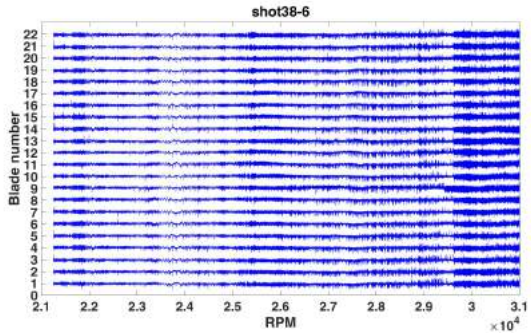

(d) 19 bars

FIGURE 9: Waterfall plots with and without bars

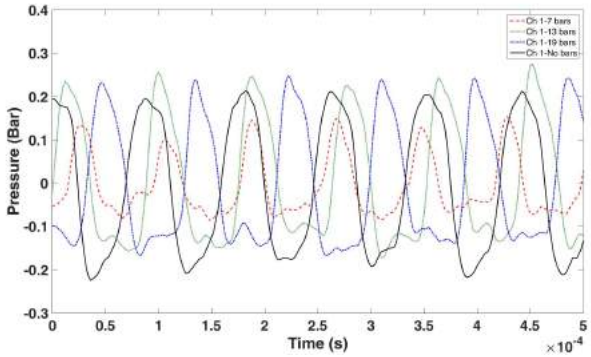

(a) Sensor 1

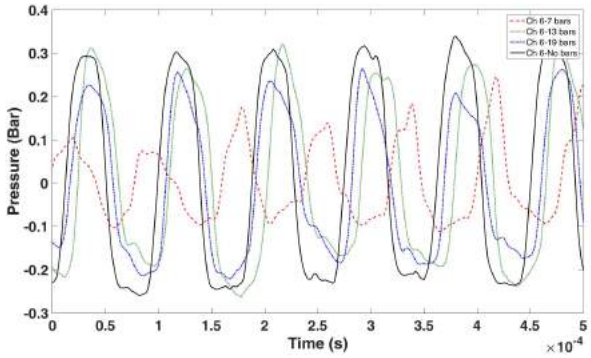

(b) Sensor 6

FIGURE 10: Pressure with and without bars

Forum and Aerospace Exposition, no. NASA NASA/TM–2002-211794 AIAA-2002-3790.

[3] Vakhtin, A. B., Chen, S., and Massick, S. M., 2009. "Optical probe for monitoring blade tip clearance". In 47th AIAA Aerospace Sciences Meeting Including The New Horizons Forum and Aerospace Exposition, no. 2009-507.

[4] Hafner, M., Holst, T., and Billington, S., 2011. "Blade tip measurement advanced visualization using a three dimensional representation". In ASME 2011 Turbo Expo: Turbine Technical Conference and Exposition, no. GT2011-46523, pp. 419–425.